Polymer 50 (2009) 3528–3536

Contents lists available at ScienceDirect

Polymer

journal homepage: www.elsevier.com/locate/polymer

Carbon nanotubes-*graft*-polyglycerol: Biocompatible hybrid materials for nanomedicine

Mohsen Adeli [a,b,*], Narjes Mirab [a], Mohammad Shafiee Alavidjeh [c], Zahra Sobhani [c], Fatemeh Atyabi [c]

[a] Department of Chemistry, Faculty of Science, Lorestan University, Khoramabad, Iran
[b] Institute for Nanoscience and Nanotechnology, Sharif University of Technology, Tehran, Iran
[c] Department of Pharmaceutical Sciences, Faculty of Pharmacy, Tehran University of Medical Sciences, Tehran, Iran

ARTICLE INFO

Article history:
Received 4 April 2009
Received in revised form
23 May 2009
Accepted 29 May 2009
Available online 3 June 2009

Keywords:
Hybrid materials
Carbon nanotube
Polyglycerol

ABSTRACT

New biocompatible and water soluble hybrid materials containing multi-wall carbon nanotubes (MWCNTs) as core and hyperbranched polyglycerol (PG) as shell were synthesized successfully. In this work, pristine MWCNTs were opened and functionalized through treatment with acid and polyglycerol was covalently grafted onto their surface by the "grafting from" approach based on in-situ ring-opening polymerization of glycidol. Some short-term In vitro cytotoxicity and hemocompatibility tests were conducted on HT1080 cell line (human Fibrosarcoma), because this epithelial cell line can be one of the first route of entry of the exogenous materials to the vascular system and therefore subsequent interactions with the whole body, in order to investigate their potential application in nanomedicine and to understand the limitation and capability of these material as nanoexcipients in biological systems.

1. Introduction

Carbon nanotubes have attracted considerable attention because of their unique atomic structure, high surface area-to-volume ratio and excellent electronic, mechanical and thermal properties [1–3]. They have a wide range of potential applications including nanoelectronic, sensors, fillers in composites materials and others [4–6]. Carbon nanotubes are also promising materials for nanomedicine. They have potential applications as carriers for delivery of drugs, RNA, DNA, peptides and other biological active molecules into cells because of the ability to cross cell membranes [7–16]. Despite the widely demonstrated potentials of CNTs in nanomedicine, research indicates these materials can potentially cause adverse effects on environment and specially health systems [17]. Hence toxicity profile of CNTs is important in biological systems. The most important factor related to the toxicity of these materials is their high hydrophobicity or poor solubility in biological mediums which increases their interactions with cells membranes and causes formation of aggregated particles and therefore heterogeneous interactions with cell components [18]. However chemical modification or functionalization of carbon nanotubes reduce their aggregations and size polydispersity and raise their solubility, leading to an increase in their biocompatibility [19–21]. Varieties of organic molecules such as polymers and dendrimers are conjugated onto the convex and tip of CNTs by chemical reactions [22–28].

Depending on the type of interactions; two methods are used to modify the CNTs by polymers. This methods are based on either physical interactions or chemical bonding and are so called "non-covalent" or "covalent" approaches respectively. Noncovalent approach is based on poor vander Waals interactions between CNTs and polymers and includes dispersion with the low molar mass polymers, polymer wrapping and polymer adsorption [29].

In the covalent approach, molecules or macromolecules are grafted onto the surface of CNTs through chemical linkages. This method is very effective because grafted macromolecules raise the solubility of CNTs even with a low degree of functionalization [30–34].

Covalent attachment of polymer chains to the surface of CNTs can be accomplished by either "grafting to" or "grafting from" methods.

In the "grafting to" method, polymers are connected to the functionalized CNTs through chemical reaction between their functional groups. The "grafting to" method is characterized by low grafting density because of the hindrance of the polymer chains which have reacted with CNTs [35].

The "grafting from" method involves the growth of polymers from the surface of CNTs by first covalently attaching of polymerization initiators and then exposing the nanotube-based macro-initiators to monomers. This method leads to the higher grafting

* Corresponding author. Department of Chemistry, Faculty of Science, Lorestan University, Khoramabad, Iran. Tel.: +98 916 3603772.
E-mail address: mohadeli@yahoo.com (M. Adeli).

0032-3861/$ – see front matter © 2009 Elsevier Ltd. All rights reserved.
doi:10.1016/j.polymer.2009.05.052

density and control over the polymer growth with the possibility of designable structure [36,37].

On the other hand among polymeric materials, dendrimers and hyperbranched polymers have attracted more interest due to their unique molecular features and properties [38–42]. Recently some hybrid materials containing carbon nanotubes and grafted hyperbranched polymers are synthesized through "grafting from" approach [43,44].

A class of hyperbranched polymers is aliphatic polyether polyols named polyglycerol with degree of branching up to 0.52–0.59 available [45,46]. PG is soluble in water freely and its biocompatibility and usefulness for biological applications such as drug delivery have been proved several years ago [47,48]. As a result combination of PG and MWCNTs leads to new functional hybrid materials with interesting properties inducted from both MWCNTs and PG. Presence of the highly biocompatible hydrophilic materials such as polyglycerol can raise the solubility of pristine MWCNTs, reduce their hydrophobicity, decrease their aggregation and size polydispersity and consequently diminish their toxicity [49,50]. On the other hand hydrophobic (MWCNT) and hydrophilic (PG) parts of these hybrid materials leads to the effective interactions with the cell membrane. Therefore in this work, MWCNTs-*g*-PG hybrid materials were synthesized and characterized and some short-term In vitro cytotoxicity and hemocopatibility tests were conducted on HT1080 cell line (human Fibrosarcoma), because this epithelial cell line can be one of the first route of entry of the exogenous materials to the vascular system and therefore subsequent interactions with the whole body, in order to investigate their potential applications of these soluble hybrid materials in different fields of nanomedicine and to understand the limitation and capability of these material as novel nanoexcipients in biological systems.

2. Experimental

2.1. Materials

Carbon nanotubes were prepared by chemical vapor deposition procedure in the presence of Co/Mo/MgO as catalyst at 900 °C. The outer diameter of MWCNT was between 20 and 40 nm. Glycidol was purchased from Aldrich. Potassium metoxid, Nitric acid, Sulfuric acid, methanol and acetone were purchased from Merck. The cell line (HT1080, ATCC) were obtained from PASTEUR institute, Tehran, Iran. MTT powder, Annexin-V FLUOS Staining Kit, LDH Kit, RPMI 1640 and FCS were obtained from Sigma, Roche, Promega, WI and Biosera respectively. Dialysis bag was purchased from Sigma.

2.2. Characterization

^{1}H NMR spectra were recorded in methanol solution on a Bruker DRX 400 MHz apparatus with the solvent proton signal for reference. ^{13}C NMR spectra were recorded on the same instrument using the solvent carbon signal as a reference. IR measurements were performed using a Nicolet 320 FTIR. Transmission electron microscopic (TEM) analyses were performed by a LEO 912 AB electron microscope. Differential scanning calorimeter (DSC) diagrams were recorded using a DSC 823-e device (Mettler toledo, Switzerland) using the following condition: linear heating rate 10 K/min from 20 to 400 °C, dynamic inert nitrogen atmosphere (10 ml/min). Thermo gravimetric analysis (TGA) was carried out in a thermal analyzer (model: DSC 60, shimadzu, Japan) under dynamic atmosphere of an inert gas (i.e. N_2) at 30 ml/min (room temperature). The particle size and polydispersity were determined using Dynamic Light Scattering (DLS) (zetasizer ZS, Malvern Instruments). The molecular weight distributions were determined by size exclusion chromatography (SEC) using Pump 1000 using PL aquagel-OH mixed- H 8 μm column connected to a differential refractometer, RI with water as the mobile phase at 25 °C. Pullulan standard samples were used for calibration.

2.3. Opening of MWCNTs

MWCNTs were purified and opened according to reported procedures in literature (Supporting information page 1) [35,37].

2.4. Synthesis of MWCNT-g-PG hybrid materials

Saturated solution of potassium methoxide in methanol (2 ml) was mixed with opened carbon nanotube (0.05 g) and mixture was placed in an ultrasonic bath for 30 min and stirred at room temperature for 1 h. Then it was refluxed at 80 °C for 2 h. Mixture was washed with dry methanol three times and solvent was removed by vacuum oven at 60 °C. Glycidol (5 ml) was added to the deprotonated MWCNT at 100 °C dropwise and mixture was stirred at 100 °C for 4 h. Then it was cooled and contents were dissolved in methanol. The product was precipitated in acetone and it was dialysis in water for 24 h. All steps of reaction were performed under nitrogen atmosphere.

2.5. Biocompatibility tests

Different methods were used to test the biocompatibility of MWCNT-*g*-PG hybrid materials (Supporting information pages 1, 2, 3 and 4).

2.6. Cell culture

Human fibrosarcoma epithelial like cell line (HT1080) was obtained from Iran Pasteur Institute (ATCC, CCL-121) and used for cell cytotoxicity studies. Cells were grown in 25 cm^2 culture flasks using RPMI 1640. Cell culture medium supplemented with 10% FCS and 1% penicillin–streptomycin at 37 c with 5% CO^2 in an incubator. The cells sub-cultured every 72 h and harvested from sub-confluent cultures (70% using 0.05% Trypsin–EDTA). The cells were cultured 10,000/well in 96-well plates in all experiments except for apoptosis and necrosis assay which we used 25 cm^2 culture flasks.

3. Result and discussion

The synthesis of water-soluble carbon nanotubes is an important topic, because they have potential applications in biology and materials science. Scheme 1 illustrates the synthetic route of MWCNT-*g*-PG hybrid materials. In this synthetic route the hyperbranched molecular trees were grown from the surface of MWCNT via in-situ anionic ring-opening polymerization.

As above mentioned, one of the most important reasons for conjugating PG trees to the surface of MWCNTs was improving their solubility in water. Expectedly PG-functionalized carbon nanotubes were completely soluble in water and polar organic solvents such as methanol whereas pristine or opened MWCNTs were not soluble in these solvents (Supporting information page 5 Figure 1).

In this work different glycidol/MWCNT Wt% ratios were used to synthesize MWCNT-*g*-PG hybrid materials with different PG thickness. The chemical structure, morphology, thermal properties, molar mass and size of MWCNT-*g*-PG hybrid materials were determined by IR, ^{13}C NMR, ^{1}H NMR, Raman spectroscopy, TEM, TGA, DSC, GPC and DLS. In the IR spectra of MWCNT-*g*-PG, the absorbance band of the hydroxyl functional groups of polyglycerol and C=C bonds of MWCNT were appeared at 3000–3500 cm^{-1} and 1630 cm^{-1} respectively (Supporting information page 5 Figure 2).

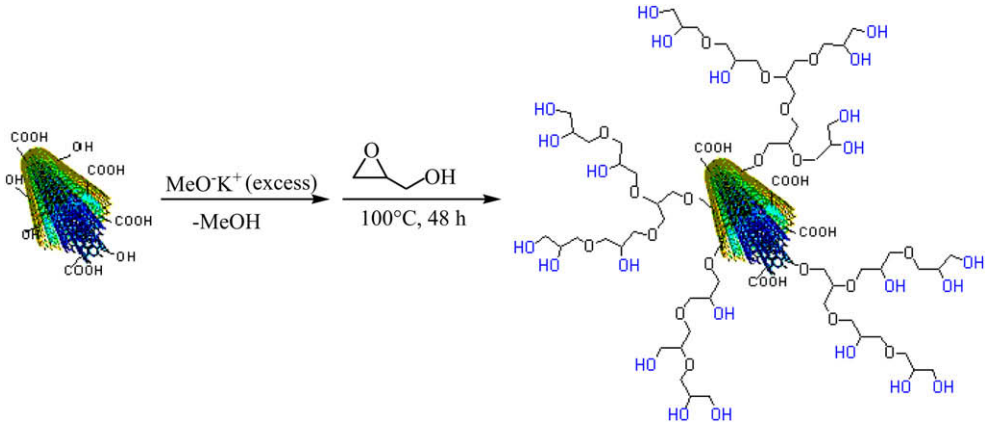

Scheme 1. Synthetic process for the MWCNT-*g*-PG hybrid materials.

The ^{1}H NMR spectrum of MWCNT-*g*-PG shows the methylene and methine protons of PG as a broad resonance between 3.1 and 3.9 ppm. A signal at 4.8 ppm is assigned to the hydroxyl protons of PG (Supporting information page 5 Figure 3).

The polyglycerol backbone consists of linear (L), dendritic (D) and terminal units (T). In the ^{13}C NMR spectrum of MWCNT-*g*-PG,(1) L_{13}: $-CH_2OH$ carbon at 62.5 ppm, CH_2 carbon at 71.3 ppm and –CHOH at 80.8 ppm.(2) L_{14}: both CH_2 carbons at 74 ppm, CHOH carbon at 70.7 ppm.(3) Terminal unit (T): CH_2OH carbon at 66.5 ppm, CHOH carbon at 72.4 ppm, and the CH_2 carbon at about 72.7 ppm; (4) dendritic unit (D): CH carbon at 80.2 ppm, one CH_2 carbon at 73.0 ppm, and the other at about 72.7 overlapping with a CH_2 carbon of a terminal unit and weak signals for C=C carbons of CNT at 129–143 ppm and 170–180 ppm can be clearly seen (Supporting information page 6 Figure 4).

Raman spectroscopy is a technique which has been widely used to the study carbon nanotubes. Fig. 1a–c illustrates the Raman spectra of pristine MWCNT, opened MWCNT and MWCNT-*g*-PG hybrid materials respectively. As it is well known there are two special bands in the Raman spectra of CNTs: the tangential bands (G bands) at 1400–1600 cm^{-1} and the disorder mode band (D bands) around 1200–1300 cm^{-1}. The D bands corresponds to defects in the

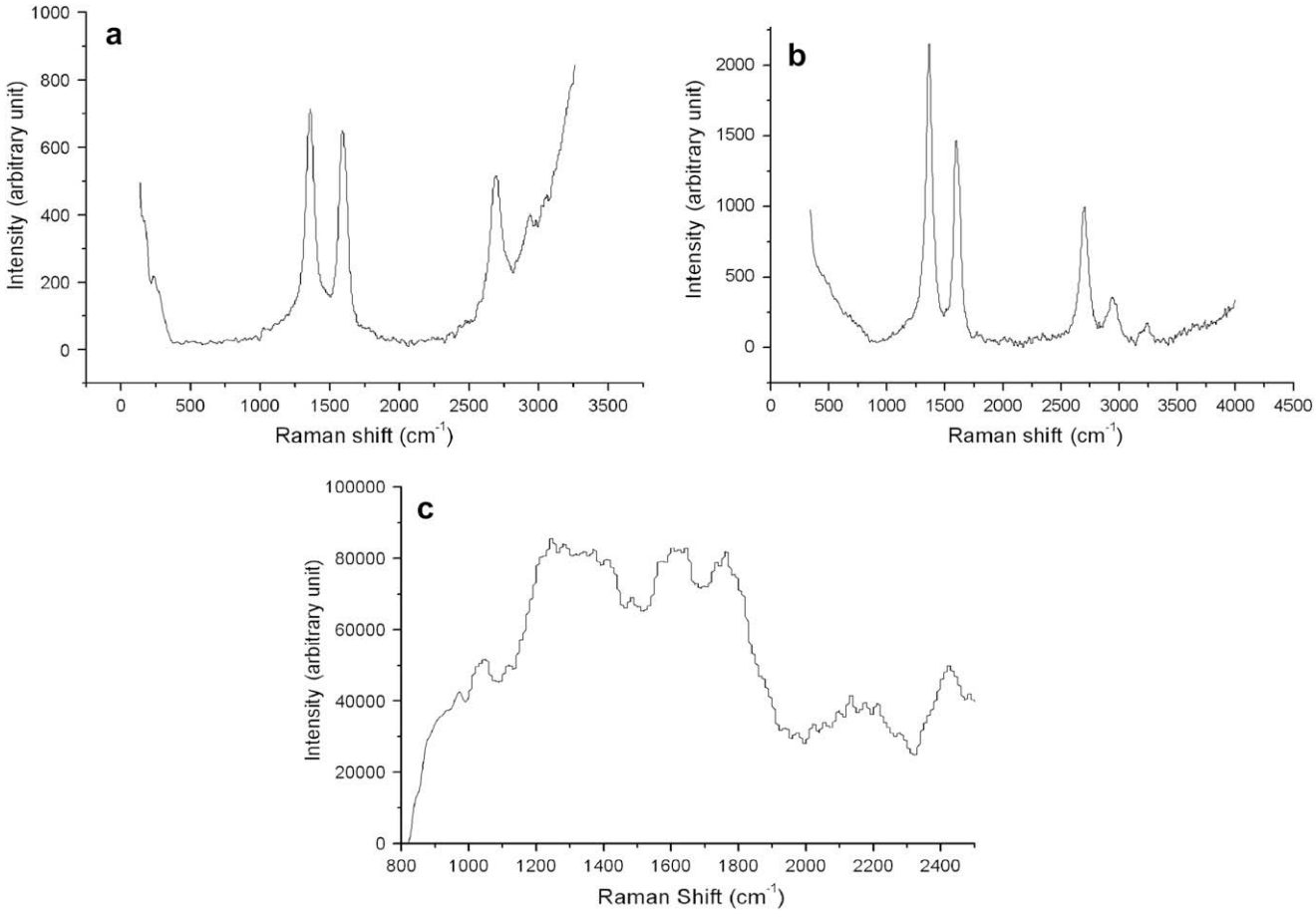

Fig. 1. Raman spectra of a) pristine MWCNT b) opened MWCNT and c) MWCNT-*g*-PG hybrid materials.

curved graphene sheet; tube ends and attributed to sp^3-hybridized carbon in the hexagonal framework of the nanotube walls, while the G bands are related to the graphitic hexagon-pinch mode. The G bands are a common feature in any carbon nanotube spectrum, appearing as multi-peak features around 1580 cm^{-1}. In Fig. 1 a clearly D bands and G bands of pristine MWCNT can be seen at 1360 cm^{-1} and 1590, respectively.

Functionalization of the carbon nanotubes result in a substantial increase in the number of sp^3-hybridized carbons with a concomitant increase in the D mode and a decrease in the tangential G mode associated with sp^2-hybridized carbons from the graphitic sidewalls. This increase in the ratio of sp^3: sp^2 is described by the I_D/I_G ratio. According to Fig. 1 I_D/I_G is 1.06 and 1.46 for pristine and opened MWNTs respectively. This indicates to increase the structural disorder of carbon nanotubes produced by functionalization.

Fig. 1c shows the Raman spectra of MWNTs-*g*-PG hybrid material. Presence of the PG shell onto the surface of the MWCNT has caused a broadening in its D bands and G bands. In this figure two broad bands around 1350 and 1580 cm^{-1} are appeared which are assigned to the sp^3- and sp^2-hybridized carbons.

TEM is a powerful tool for characterizing nanomaterials such as CNTs and polymer-functionalized CNTs. Fig. 2a shows the TEM image of pristine MWCNTs in which catalytic nanoparticles used to synthesize carbon nanotubes are still remained in their tips and backbone. Fig. 2b shows the TEM image of opened MWCNTs. In this figure the opened capes of carbon nanotubes can be clearly seen. Fig. 2c displays the TEM image of MWCNT-*g*-PG synthesized using glycidol/MWCNT = 5 ratio. Dispersed MWCNTs in the polyglycerol matrix can be seen clearly. According to TEM experiments it seems grafting of the PG shell on the surface of MWCNTs causes an extra

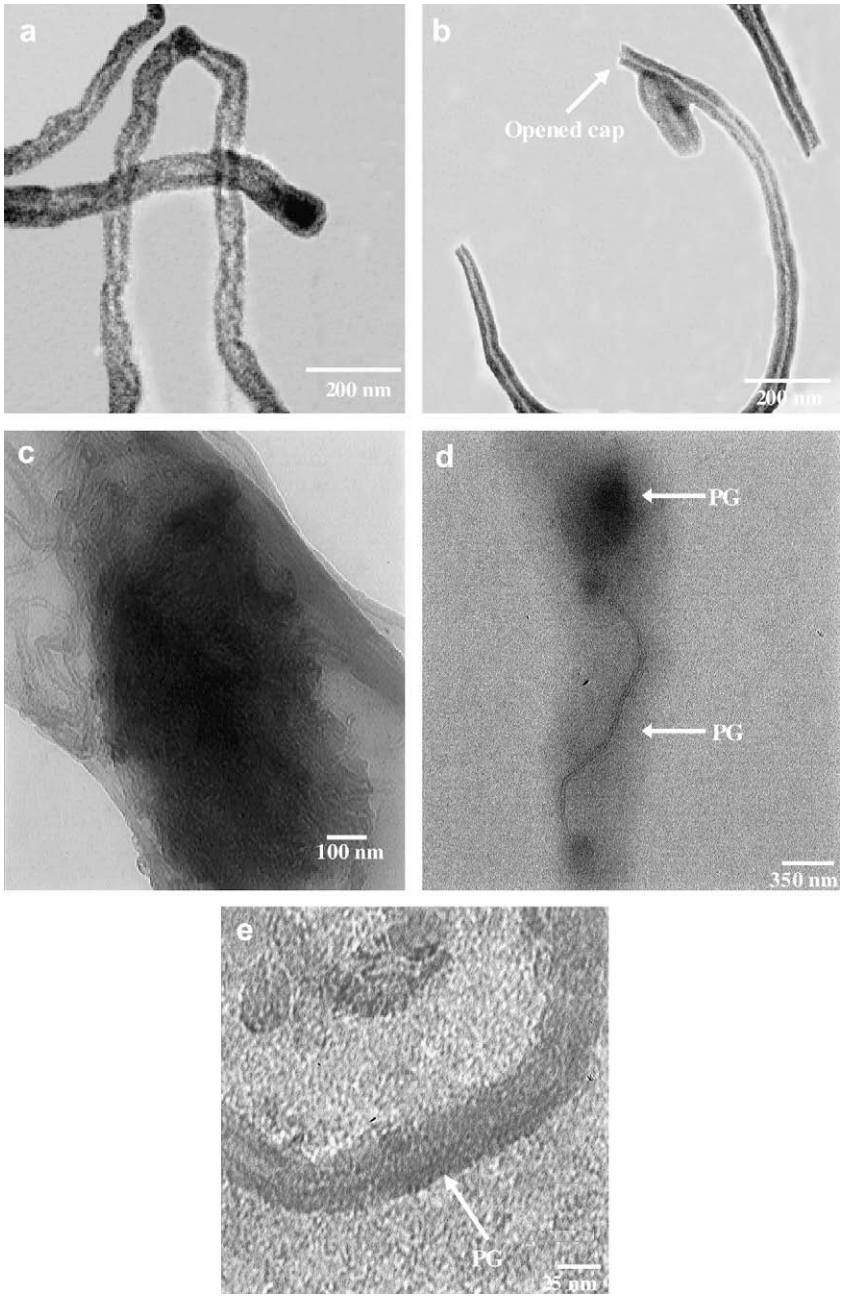

Fig. 2. TEM images of a) pristine MWCNT b) opened MWCNT c) MWCNT-*g*-PG hybrid materials d) a single MWCNT-*g*-PG and e) higher magnification of a single MWCNT-*g*-PG.

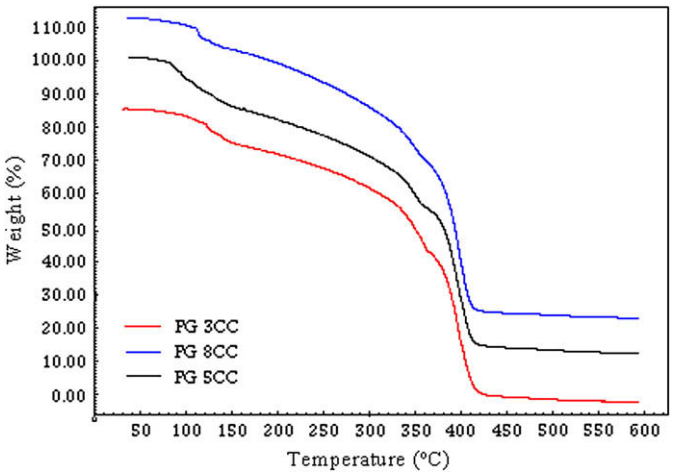

Fig. 3. TGA diagrams of MWCNT-*g*-PG hybrid materials synthesized using a) 3, b) 5 and c) 8 glycidol/MWCNT Wt% ratio.

flexibility in their structure. Fig. 2d shows a single MWCNT-*g*-PG in which the dark parts are related to the grafted PG onto the MWCNT. The intensity of the dark color on the tips of MWCNT is relatively higher than sidewalls implying to the higher density of grafted PG on these regions. Higher intensity of PG on the tips of MWCNT can be explained by higher density of hydroxyl functional groups in these regions. This result is in agreed with reported results in literatures because tips of CNTs are containing pentagonal rings which are more reactive. In Fig. 2d MWCNT is surrounded by a continued shell. This result show that instead several big PG branches (high DP), PG growths on the surface of MWCNT as a large number of small PG branches (low DP). Fig. 2e shows an image of MWCNT-*g*-PG with higher magnification. In this figure a dense continued layer of PG with a thickness around 7 nm on the surface of carbon nanotube is presented. The polyglycerol as a soft shell and MWCNT as a hard core are clearly discerned.

The TGA measurements provided further evidence regarding the content and species of grafted polymer on the surfaces of CNTs because they have different thermal-stability. Fig. 3 shows the TGA thermograms of MWCNT-*g*-PG hybrid materials synthesized using 3, 5 and 8 glycidol/MWCNT ratios. The TGA curve of MWCNT-*g*-PG hybrid material presents two weight-loss regions. The first one (between 100 and 360 °C) is assigned to the polymer chain while the second one (above 360 °C) is related to the depletion of carbon nanotube with diverse diameters. The plateau in the TGA trace after 450 °C was attributed to carbon nanotube. In this figure the decomposition temperature region (T_d) and also the PG content for all hybrid materials is almost the same (Table 1). This result shows that the PG content of hybrid materials do not depend on the monomer feed ratio. Confirming the TEM results, it seems the MWCNT surface is containing a large number of initiator sites which are close together and due to the steric hindrance between small packed PG branches after a short time polymerization is stopped. Hence it is believed that MWCNTs are containing a large

Table 1
Weight-loss at 400 °C for different MWCNT-*g*-PG hybrid materials synthesized using different glycidol/MWCNT Wt% ratios.

Glycidol/MWCNT Wt% ratios	PG content
3	55
5	56
8	56

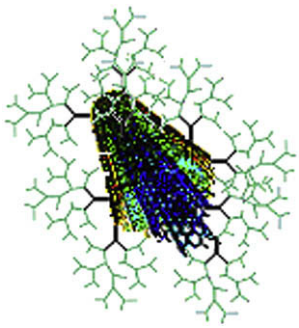

Fig. 4. Simultaneous growth of a large number of PG branches on the surface of MWCNT causes steric hindrance between them so that each MWCNT is containing a large number of small PG branches.

number of PG branches with low DP. On the other hand the end alkoxide groups which are responsible to attack to epoxy ring of monomer can abstract the proton of glycidol and transfer the anionic center from MWCNT-*graft*-PG to monomer. The result of this reaction is to quench grafted PG branches, decreasing their DP and obtaining a hybrid material containing a central MWCNT and a large number of small PG branches (Fig. 4). In order to evaluate this proposal the time of polymerization was changed and molecular weight and PG content of synthesized MWCNT-*graft*-PG hybrid materials was determined. Results showed that there was not dependence between the time of polymerization and molecular weight and PG content of synthesized MWCNT-*g*-PG hybrid materials (Fig. 5).

More information about thermal stability and behavior of the MWCNT-*g*-PG hybrid materials was obtained using DSC experiments.

Fig. 6 show the DSC thermograms of MWCNT-*g*-PG hybrid materials synthesized using 3, 5 and 8 glycidol/MWCNT ratios. Two endothermic peaks around 100–140 °C and 200–400 °C are presented in this figure. These results are in agreed with the results of TGA experiments. The first endothermic peak is assigned to the losing of water and then hydroxyl end functional groups and the second one indicate the losing of polymer backbone. Again here the thermal behavior of MWCNT-*g*-PG hybrid materials synthesized using 3, 5 and 8 glycidol/MWCNT ratios is similar.

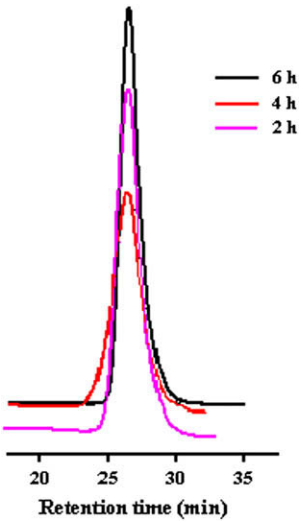

Fig. 5. GPC diagrams of synthesized MWCNT-*g*-PG hybrid materials in different polymerization times.

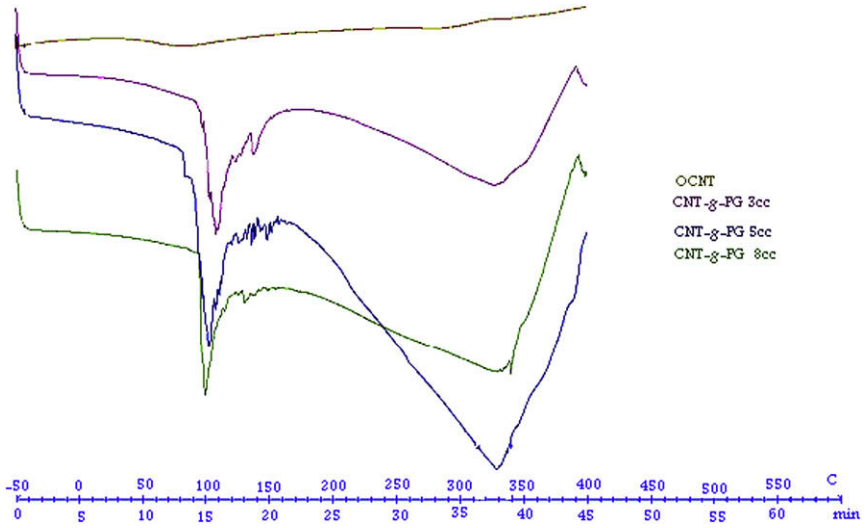

Fig. 6. DSC diagrams of a) pristine and MWCNT-*g*-PG hybrid materials synthesized using b) 3, c) 5 and d) 8 glycidol/MWCNT Wt% ratio.

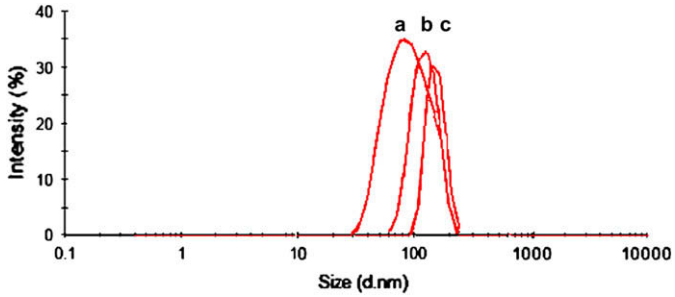

Fig. 7. DLS diagrams of MWCNT-*g*-PG hybrid materials synthesized using a) 3, b) 5 and c) 8 glycidol/MWCNT Wt% ratios.

Dynamic light scattering (DLS) was used to determine the dynamic diameter and size distributions of the polymer-functionalized MWCNTs. According to these experiments the main dynamic diameter of MWCNT-*g*-PG synthesized using 3, 5 and 8 glycidol/MWCNT ratios was almost the same and around 100 nm. Clearly there is a big difference between the measured dynamic diameter for hybrid materials and expected dynamic diameter for pristine MWCNT, the length of used MWCNTs is several micrometers. The measured diameter by DLS is actually the average dynamic diameter of hybrid materials in a special conformation in the solution sate. In the other words the recorded diameter by DLS is estimated diameter for nanotube cradling. Hence it seems noncovalent interactions (such as hydrogen bonding) between end hydroxyl functional groups of conjugated PG in different regions of a MWCNT causes a flexibility in its structure and decreasing its measured dynamic diameter in water (Fig. 7).

The biocompatibility of synthesized MWCNT-*g*-PG hybrid materials was investigated using different short term In vitro tests. The results of the MTT assay, as an indicator of mitochondrial function, showed no sign of toxicity up to 1 mg/ml concentration after 24 h incubation and data were not significant ($p < 0.05$). Except for 0.25 mg/ml concentration in which growth of the treated cells increased in compare to the untreated control ones (136% growth against negative control), the same results were obtained after 48 h incubation (Fig. 8).

Crystal violet staining assay is a colorimetric method based on counting the adherent and almost functional cells which can uptake the dye. The results of crystal violet staining assay after 24 and 48 h incubation are shown in Fig. 9. Based on these results no sign of toxicity up to 0.5 mg/ml concentration was observed after

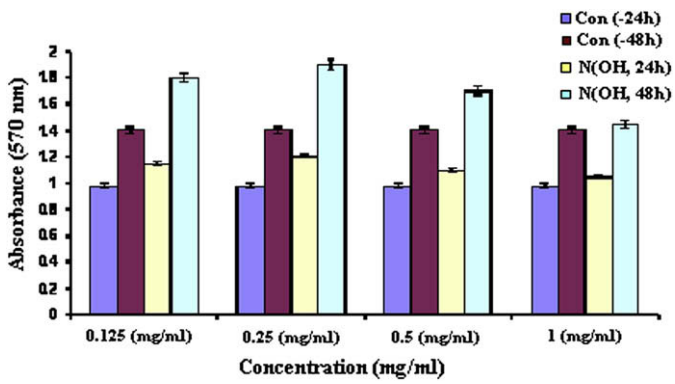

Fig. 8. Effect of concentration and time on the viability of HT1080 cell line after 24 and 48 h incubation (MTT assay).

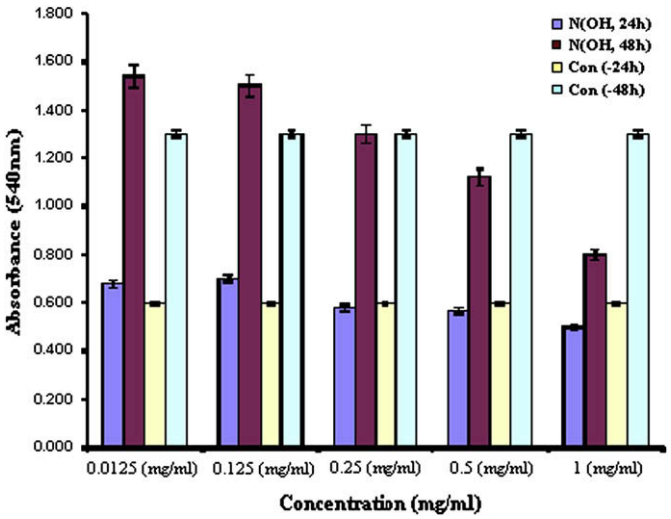

Fig. 9. Effect of concentration and time on functionality of HT1080 cell line after 24 and 48 h incubation (crystal violet staining assay).

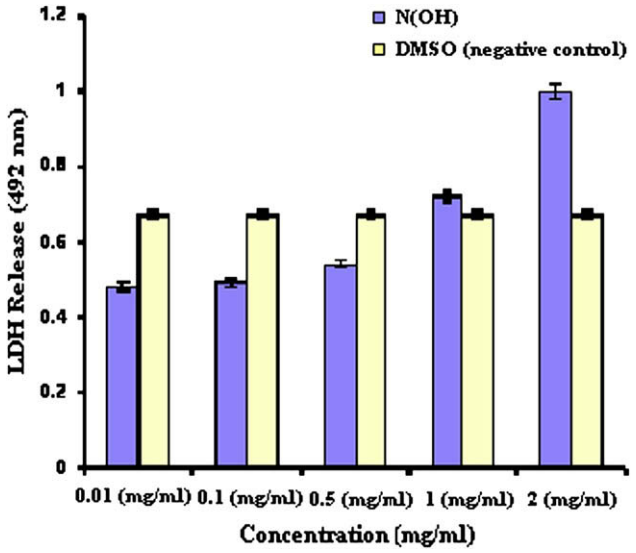

Fig. 10. Effect of concentration on cell membrane integrity after 24 h incubation.

24 h incubation while 1 mg/ml concentration showed toxicity against the controlled medium after this time (83% diminish against negative controlled cells). However for 0.125 mg/ml concentration, cell viability increased after 24 h incubation. Any statistical difference was not shown up to 0.5 mg/ml concentration after 48 h incubation. Considerable toxicity for 1 mg/ml concentration was observed after this time (61% decreasing against control).

Fig. 10 shows LDH results for treated cells against 0.1% v/v DMSO, as negative control, after 24 h incubation. Based on these results, only for 2 mg/ml concentration a considerable toxicity was observed (150% increasing against 0.1% v/v DMSO as negative control, $p < 0.05$).

Annexinv-PI assay is a test that differentiates early apoptosis and necrosis (secondary apoptotic cells). Fig. 11 shows Annexinv-PI assay results in which a concentration-dependent behavior in the number of apoptotic and necrotic cells is observed so that there is an about 7- and 2-fold increase in the number of apoptotic and necrotic cells from the lowest to highest concentration respectively. According to these data the number of necrotic and apoptotic cells are negligible even in the highest concentrations ($p < 0.05$).(Supporting information page 6 and 7 Figure 5.)

Hemolysis assay showed no sign of harsh hemolysis (less than 9%) up to 1 mg/ml concentration within 2 h of incubation (Supporting information page 7 Figure 6).

Any unnatural changes in the morphology of cells were not seen up to the 1 mg/ml concentration (Fig. 12).

As a result, crystal violet staining test and LDH assay showed a dose and time-dependent toxicity profile at used concentrations whereas MTT and hemolysis assays didn't show statistical difference in compare to negative control up to 1 mg/ml concentration. These observations can be ascribed by a variety of reasons such as chemical and physical interactions between samples and cellular components or cell membranes [51].

On the other hand aggregations of samples in high concentrations in aqueous physiologic media [52] which can induce heterogenous interaction with the cell membrane cause more toxicity. Another factor is increased hydrophobicity which is the result of alignment structure of particles at higher concentrations. This

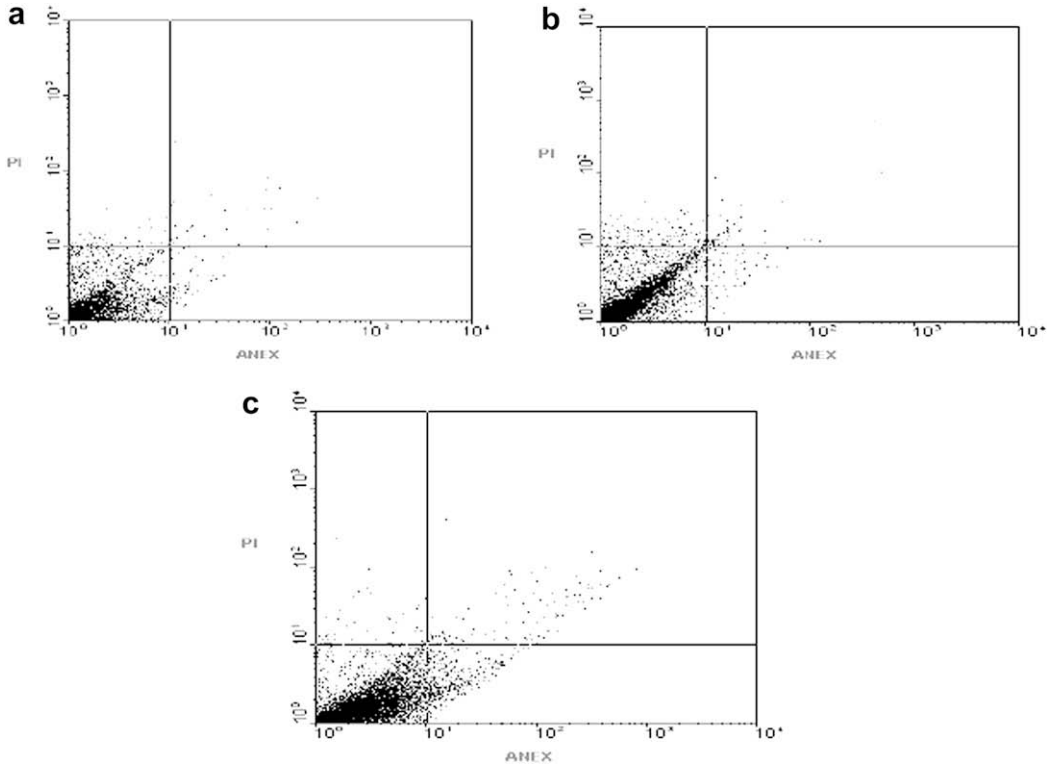

Fig. 11. Dot plots of AnnexinV-FITC/PI staining of HT1080 cells after 24 h incubation. Three phenotype can be observed: viable (lower left quadrant); apoptotic (lower right quadrant), and necrotic or secondary apoptotic (upper right quadrant). a) Untreated cells, b) cells treated by 0.35 mg/ml of MWCNT-*graft*-PG hybrid materials and c) cells treated by 0.7 mg/ml of MWCNT-*graft*-PG hybrid materials.

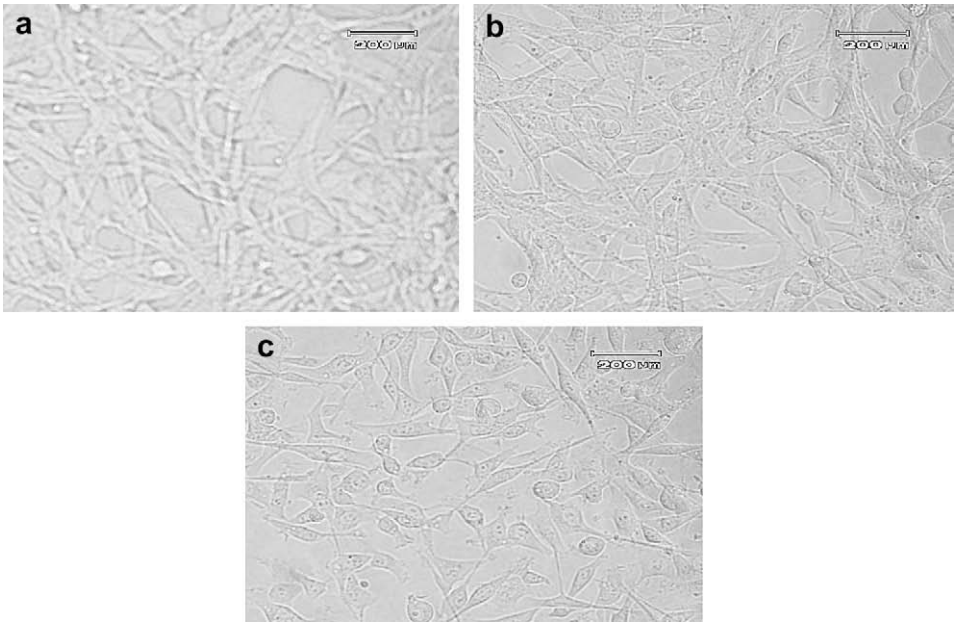

Fig. 12. Effects of two different concentration of MWCNT-*g*-PG hybrid materials (0.35 mg/ml and 0.7 mg/ml) on morphology of cells after 24 h incubation. a) Untreated control cells, b) cells treated by 0.35 mg/ml of MWCNT-*graft*-PG hybrid materials and c) cells treated by 0.7 mg/ml of MWCNT-*graft*-PG hybrid materials.

factor causes more interactions with the cell membrane and more ability to enter the lipidic bilayer cell membrane.

Ratio of apoptosis to necrosis is another factor which depends on concentration [51,53]. In the case of synthesized hybrid materials the ratio of apoptosis to necrosis depends on the concentration directly and it is about 3.5/1 at higher concentration (0.7 mg/ml) which is an advantage for these systems. Everybody knows that in the case of necrosis process materials can be liberated from the lysed cells instantly, in opposite to apoptosis, which can induce instant unwanted inflammatory responses and subsequent harmful reactions which are not good at all in particle designing and biocompatibility issues. These adverse reactions are not seen for apoptosis process, in that the living organism has time to identify (e.g., translocation of phosphatidyl serine to the outer membrane of the cell wall), treat and scavenge the cell debris before causing any harmful side effects in its natural. Our next step is to make clear the exact mechanism contributing to toxicity of these materials at higher concentrations and to conduct in vivo experiments to gain information about the pharmacokinetics of these hybrid materials.

4. Conclusion

In summary, MWCNTs can be successfully modified using highly branched polyglycerol through ring opening polymerization of glycidol onto their surface. Due to their high biocompatibility and water solubility, MWCNT-*g*-PG hybrid materials are promising materials in order to use in the biological systems. According to the results of In vitro cytotoxicity tests and hemolysis assay, we did not see any adverse effects on the HT1080 cell and also red blood cells up to 1 mg/ml concentration. Hence the result of functionalization of carbon nanotube by polyglycerol is to decrease in vitro cytotoxicity of carbon nanotube. Although MWCNT-*g*-PG hybrid materials could be considered as biocompatible materials and are candidates for various applications in nanomedicine field potentially, long-term in vitro toxicity experiments and preclinical in vivo studies are necessary in order to illustrate their toxicity profile for future biomedical applications.

Acknowledgment

Authors would like to thank "Iranian Nanotechnology Initiative" in order to support this work financially.

Appendix A. Supplementary data

Supplementary data associated with this article can be found in the online version, at doi:10.1016/j.polymer.2009.05.052.

References

[1] Dresselhaus M, Dresselhaus G, Avouris P. Carbon nanotubes: synthesis, properties and applications. 1st ed. Berlin: Springer-Verlag; 2001.
[2] Balasubramanian K, Burghard M. Analytical and Bioanalytical Chemistry 2006;385:452–68.
[3] Tasis D, Tagmatarchis N, Bianco A, Prato M. Chemical Reviews 2006;106:1105–36.
[4] Martel R. ACS Nano 2008;2:2195–9.
[5] Wu Y, Phillips JA, Liu H. ACS Nano 2008;2:2023–8.
[6] Qiu JD, Zhou WM, Guo J, Wang R, Liang RP. Analytical Biochemistry 2009;385:264–9.
[7] Kam NWS, Liu Z, Dai H. Journal of American Chemical Society 2005;127:12492–3.
[8] Singh R, Pantarotto D, Lacerda L, Pastorin G, Klumpp C, Prato M, et al. Proceedings of the National Academy of Sciences U S A 2006;103:3357–62.
[9] Krajcik R, Jung A, Hirsch A, Neuhuber W, Zolk O. Biochemical and Biophysical Research Communications 2008;369:595–602.
[10] Prato M, Kostarelos K, Bianco A. Accounts of Chemical Research 2008;41:60–8.
[11] Yarotski DA, Kilina SV, Talin AA, Tretiak S, Prezhdo OV, Balatsky AV, et al. Nano Letters 2009;9:12–7.
[12] Lacerda L, Raffa S, Prato M, Bianco A, Kostarelos. Nano Today 2007;2:38–43.
[13] Lacerda L, Bianco A, Prato M, Kostarelos K. Advanced Drug Delivery Reviews 2006;58:1460–70.
[14] Yang X, Zhang Z, Liu Z, Ma Y, Yang R, Chen Y. Journal of Nanoparticle Research 2008;10:815–22.
[15] Liu Zh, Sun X, Nakayama-Ratchford N, Dai H. ACS Nano 2007;1:50–6.
[16] Guo Y, Shi D, Cho H, Dong Z, Kulkarni A, Pauletti GM, et al. Advanced Functional Materials 2008;18:1–9.
[17] Maynard AD, Baron PA, Foley M, Shvedova AA, Kisin ER, Castranova V. Journal of Toxicology Environmental Health, Part A 2004;67:87–107.
[18] Ding L, Stilwell J, Zhang T, Elboudwarej O, Jiang H, Selegue JP, et al. Nano Letters 2005;12:2448–64.
[19] Tsubokawa N. Polymer Journal 2005;37:637–55.
[20] Zhang LW, Zeng L, Barron AR, Monterio-Riviere NA. International Journal of Toxicology 2007;161:135–42.
[21] Zeineldin R, Al-Haik M, Hudson LG. Nano Letters 2009;9:751–7.

[22] Feng Q, Xie X, Liu Y, Zhao W, Gao Y. Journal of Applied Polymer Science 2007;106:2413–21.
[23] Campidelli S, Sooambar C, Diz EL, Ehli C, Guldi DM, Prato M. Journal of American Chemical Society 2006;128:12544–52.
[24] Yingkui Y, Xiaolin X, Zhifang Y, Xiaotao W, Wei C, Yiu-Wing M. Macromolecules 2007;40:5858–67.
[25] Wang L, Jiang G, Chen Ch, Dong X, Chen T, Yu H. Material Letters 2005;59:2085–9.
[26] Qiao R, Ke PC. Journal of American Chemical Society 2006;128:13656–7.
[27] You YZ, Hong CY, Pan CY. Journal of Physical Chemistry C 2007;111. 16161–6.
[28] Baskaran D, Mays JW, Bratcher MS. Angewandte Chemie International Edition 2004;43:2138–42.
[29] Liu P. European Polymer Journal 2005;41:2693–703.
[30] Dalton AB, Stephan C, Coleman JN, McCarthy B, Ajayan PM, Lefrant S. Journal of Physical Chemistry B 2000;104:10012–6.
[31] Chen RJ, Zhang Y, Wang D, Dai H. Journal of American Chemical Society 2001;123:3838–9.
[32] Star A, Stoddart JF, Steuerman D, Diehl M, Boukai A, Wong EW. Angewandte Chemie International Edition 2001;40:1721–5.
[33] Chen J, Liu H, Weimer WA, Halls MD, Waldeck DH, Walker GC. Journal of American Chemical Society 2002;124:9034–5.
[34] Narizzano R, Nicolini C. Macromolecular Rapid Communications 2005;26:381–5.
[35] Sepahvand R, Adeli M, Astinchap B. Journal of Nanoparticle Research 2008;10:1309–18.
[36] Qin S, Qin DQ, Ford WT, Resasco DE, Herrera JE. Journal of American Chemical Society 2004;126:170–6.
[37] Adeli M, Bahari A, Hekmatara H. Nano: Brief Reports and Reviews 2008;3: 37–44.
[38] Namazi H, Adeli M, Zarnegar Z, Jafari S, Dadkhah A, Shukla A. Colloid and Polymer Science 2007;285:1527–33.
[39] Adeli M, Zarnegar Z, Kabiri R. European Polymer Journal 2008;44: 1921–30.
[40] Namazi H, Adeli M. Journal of Polymer Science, Part A: Polymer Chemistry 2005;43:28–41.
[41] Adeli M, Zarnegar Z, Dadkhah A, Hossieni R, Salimi F, Kanani A. Journal of Applied Polymer Science 2007;104:267–72.
[42] Namazi H, Adeli M. Polymer 2005;46:10788–99.
[43] Xu Y, Gao Ch, Kong H, Yan D, Zhang Jin Y, Watts. Macromolecules 2004;37:8846–53.
[44] Gao Ch, Muthukrishnan Sh, Li W, Yuan J, Xu Y, Müller A. Macromolecules 2007;40:1803–15.
[45] Haag R, Sunder A, Stumbe JF. Journal of American Chemical Society 2000;122:2954–5.
[46] Adeli M, Haag H, Zarnegar Z. Journal of Nanoparticle Research 2007;9:1057–65.
[47] Frey H, Haag R. Reviews in Molecular Biotechnology 2002;90:257–67.
[48] Calderón M, Warneckeb A, Gärser R, Haag R, Kratz F. Journal of Controlled Release 2008;132. e54–5.
[49] Kainthan RK, Hester SR, Levin E, Devina DV, Brooks DE. Biomaterials 2007;28:4581–90.
[50] Zhao B, Hu H, Yu A, Perea D, Haddon RC. Journal of American Chemical Society 2005;127:8197–203.
[51] Cui DX, Tian FR, Ozkan CS, Wang M, Gao H. Journal of Toxicology Letters 2005;155:73–85.
[52] Nimmagadda A, Thurston K, Nollert MU, Mcfetridge PS. Journal of Biomedical Materials Research Part A 2006;76:614–25.
[53] Jia G, Wang H, Yan L, Wang X, Pei R, Yan T, et al. Environmental Science Technology 2005;39:1378–83.